TR-O-0069

49

GaAs選択エッチング用 $HF+H_2O_2+H_2O$混合液の基本特性

武部　敏彦

1994. 3. 31

ATR光電波通信研究所

ATR Technical Report

報告題名　：　GaAs選択エッチング用$HF+H_2O_2+H_2O$混合液の基本特性

報告者　：　武部　敏彦

所属　：　ATR光電波通信研究所　通信デバイス研究室

報告内容概要　：

【1】研究の動機

多種多様な半導体技術の中で、化学エッチングは材料の基礎研究のみならずデバイス作製にも欠かせない基本的技術である。ガリウム砒素(GaAs)はIII-V族化合物半導体の一員で、超高速電子デバイスや高効率光デバイス用の基本材料として広く研究されている。従来のGaAsのエッチング液に関する研究のほとんどは、広くデバイス応用に供されている(001)面に対するエッチング特性のみを対象としてきた。しかし近年、(001)面以外の面方位を有する基板やいろいろの面方位が共存するパターン基板上で、表面特性の異方性を利用した結晶成長、微細構造形成、デバイス作製に関する研究が成されるようになってきた。

本報告は、これらの広い応用に適した新しいGaAsエッチング液、$HF+H_2O_2+H_2O$混合液、を初めて開発し、その(001)、(110)、(111)B、及び(111)A面上でのエッチング特性をエッチング液の組成に対し系統的に調べた結果を報告するものである。

【2】研究の成果

1. H_2O_2過剰の$HF+H_2O_2+H_2O$混合液は、H_2OとH_2O_2の量で制御される以下の様な優れた選択エッチング特性を示した。

(1) $[\bar{1}\bar{1}\bar{1}]$B方向のエッチング速度の[111]A方向のエッチング速度に対する比を異方性パラメータγ、とすると、組成に応じて3.8から0.9まで変化させることができる。エッチング速度は、ほとんどの組成で

[111]A方向に最低値を示すが、高H_2O·低H_2O_2濃度では[$\bar{1}\bar{1}\bar{1}$]B方向に最低値を示すようになる。[111]A方向以外でエッチング速度が最低値を示すのは本混合液が初めてである。

(2) 低H_2O·高H_2O_2濃度では結晶の異方性を強く反映したエッチングプロファイルを示し、高H_2O·低H_2O_2濃度では基板面方位に依らない等方的なエッチングプロファイルを示す。

(3) すべての基板面方位に対して、基板面と側壁の成す角度を連続的かつ広範囲に変化させることができる。

(4) エッチングプロファイルは、エッチング速度の異方性と、(111)A面は他の面とシャープに交差するが、($\bar{1}\bar{1}\bar{1}$)B面は緩やかに交差するという対照性とに深く関連している。

2. 本混合液のエッチング特性は、HFがGa酸化物を選択的に溶解しH_2OがAs酸化物を選択的に溶解する、というモデルで説明できた。

3. 本混合液の特性を従来のエッチング液の特性と詳細に比較し、その特徴を明らかにした。

4. HF過剰の$HF+H_2O_2+H_2O$混合液はエッチング速度が極めて低く、エッチングパターンを侵食するので選択エッチングに向かない。

以上

目次

FUNDAMENTAL SELECTIVE ETCHING CHARACTERISTICS OF $HF+H_2O_2+H_2O$ MIXTURES FOR GaAs

-ABSTRACT-

Selective etching characteristics of $HF+H_2O_2+H_2O$ mixtures have been investigated for GaAs (111)A, $(\bar{1}\bar{1}\bar{1})$B, (001), and (110) surfaces. Mixtures with excess H_2O_2 have shown excellent selective etching characteristics controlled by the H_2O and H_2O_2 contents for extensive practical applications. The lowest etching rate in directions other than [111]A has been achieved with the present mixture system. Etching profiles strongly reflecting crystallographic anisotropy have been produced for low H_2O and high H_2O_2 concentrations, while those for high H_2O and low H_2O_2 concentrations have shown similar isotropic features irrespective of the substrate orientation. A continuous and extensive control of the intersection angle between the side wall and the substrate surface has been successfully achieved on all substrates. The etching profile and its dependence on the mixture composition for the four substrates have been discussed in detail in connection with the degree of anisotropy of the etching rate and the contrast that the (111)A plane sharply intersects with other planes while the $(\bar{1}\bar{1}\bar{1})$B plane has a round intersection corner. The etching characteristics of the mixture have been discussed based on the special chemical properties of HF and H_2O and compared with those of other mixture systems.

Key words : chemical etching, gallium arsenide, semiconductor,
etching anisotropy, etching profile.

I. INTRODUCTION

Among a variety of semiconductor technologies, chemical etching is a fundamental technique indispensable for basic material research and device application. Gallium arsenide (GaAs), one of the III-V compounds, has widely been studied as a basic material for high-speed electronic devices and high-efficiency optical devices. Many reports have been published on selective chemical etching systems for GaAs. They include $H_2SO_4+H_2O_2+H_2O$ [1,2,12], $NH_4OH+H_2O_2+H_2O$ [3,4,12], $H_3PO_4+H_2O_2+H_2O$ [5,12], Br_2+CH_3OH [6,7,12], $HF+HNO_3+H_2O$ [8,12], buffered $HF+H_2O_2+H_2O$ [9,10], and $C_3H_4(OH)(COOH)_3+H_2O_2$ [11]. Almost all of the reports focus primarily on etching behaviors on the (001) surface because this surface has been traditionally used for device applications. In recent years, however, there has been an increasing number of research work on crystal growth, microstructure formation, and device fabrication on substrates with orientations other than (001) [13-16] and substrates composed of various surface orientations (namely patterned substrates) [17-19]. The aim of these works is to understand and efficiently utilize the electronic, optical, lattice, and impurity incorporation properties and the crystallographic symmetries different from those of the (001) substrate. Some reports describe etching characteristics in orientations other than (001) [1,5,6,11] but provide no adequate information on the control of etching rate and profile.

In this paper, excellent selective etching characteristics of $HF+H_2O_2+H_2O$ mixtures which can cover wide applications are demonstrated for the first time on the basis of systematic experiments using various mixture compositions on substrates with different orientations. This type of mixture system has previously been used only for revealing dislocation etch-pits [20,21]. We paid special attention to orientations of side wall surfaces produced by selective etching, which have been ignored in previous papers, because their control is essential in recent applications.

II. EXPERIMENT

Silicon-doped n-type HB GaAs substrates with orientations of (001), (110), $(\bar{1}\bar{1}\bar{1})$B, and (111)A and carrier concentrations of $1\text{-}3\times10^{18}$ cm^{-3} were used for etching experiments. After degreasing in organic solvents, wafers were spin-coated with an AZ1350J resist and baked at 85 °C for 30 min in a flow of N_2 gas. The resultant resist thickness was around 1.9 μm. Stripes of 100 μm width running in the $[\bar{1}10]$ direction common to the four substrates and in the directions perpendicular to them were photolithographically patterned. The wafers were then scribed into 10 mm×6 mm pieces as etching samples. Commercial 46 weight % HF and 35 weight % H_2O_2 of semiconductor grade were used throughout together with deionized water of 17 MΩcm for dilution. In order to systematically investigate selective etching characteristics, mixtures with various HF to H_2O_2 mole ratios, α=0.05/0.34, 0.05/0.17, 0.05/0.09, 0.05/0.04, 0.25/0.11, and 0.69/0.02 were examined under wide-range dilution by H_2O from 1.2 to 56.8 mol. Here, the H_2O content involved in the HF and H_2O_2 was also taken into account in evaluating the H_2O concentration in the mixture [22]. The resist on the wafers was hardened by baking at 120 °C for 30 min in a flow of N_2 gas for etching protection. Etching was done at 25 °C, under room light, and with continuous sample stirring for uniform etching. Etching was also done at 10 °C and 40 °C for selected mixture compositions in order to investigate the temperature dependence of the etching characteristics. After etching, the sample was thoroughly rinsed in deionized water and then the resist was removed in acetone. Then, the sample was subjected to etching depth measurements with a profilometer for determination of the etching rate, R, and observation of the top and cross-sectional views of the etching profiles by scanning electron microscopy (SEM). Very good etching uniformity and reproducibility were confirmed.

III. RESULTS AND DISCUSSION

Since the etching depth was directly proportional to the etching time, R could be defined for all the compositions examined. Etching anisotropy regarding the crystallographic orientation was represented by the ratio, γ, of R in the $[\bar{1}\bar{1}\bar{1}]$B direction to that in the [111]A direction[2,5,6]. We will hereafter refer to an expression of R in the [lmn]X direction as R[lmn]X.

1. H_2O_2-excess mixtures (α=0.05/0.34, 0.05/0.17, 0.05/0.09, and 0.05/0.04)

Excellent selective etching characteristics and their controllability have been obtained for H_2O_2-excess mixtures as described below.

1-1 Etching rate

Figure 1 shows variations of R and γ with the H_2O content, [H_2O], for the mixtures with α=0.05/0.17 and 0.05/0.34. R and γ for both mixtures decrease as [H_2O] increases. The first point to be noted is that R[111]A is the lowest of all and the three other Rs show similar values. This is a feature commonly observed for all the mixtures examined except for α=0.05/0.04 and also for other etching systems[1-3,5,6,11]. The second point is that there is, in fact, a difference among the magnitudes of R[001], R[110], and R$[\bar{1}\bar{1}\bar{1}]$B and the order with respect to the magnitude changes with [H_2O]. In order to clearly demonstrate this point, we adopt values of R normalized with respect to the maximum value at each [H_2O]. Figure 2 shows the variation of normalized R with [H_2O] for the two mixtures. It is clearly recognized that the relative magnitude of R[111]A grows with [H_2O]. According to the relative magnitudes of the three other Rs, the whole [H_2O] region can be classified into three regions : For low [H_2O], we have R[110]>R$[\bar{1}\bar{1}\bar{1}]$B>R[001] and, for medium [H_2O], R[110]≈R$[\bar{1}\bar{1}\bar{1}]$B≈R[001]. R[111]A is extremely low in these [H_2O] ranges. For high [H_2O], we have R[001]>R[110]>R$[\bar{1}\bar{1}\bar{1}]$B. In this [H_2O] range, R[111]A becomes close to the three other Rs. The region criteria, the values of γ, and the etching rate order for the three regions are summarized in the first three rows of Table 1.

A comparison of Figure 2(a) and (b) indicates that each region shifts to the higher [H_2O] side as [H_2O_2] increases with no appreciable shift of the R[111]A curve. Figures 1 and 2 suggest that a further increase in [H_2O] or a further decrease in [H_2O_2] may yield γ closer to unity. Since a futher increase in [H_2O] requires an impracticably large amount of H_2O, we tried to obtain such γ by further reducing [H_2O_2] (α=0.05/0.09 and 0.05/0.04). Figure 3 plots R and γ in (a) and normalized R in (b) against [H_2O_2] with a fixed [H_2O]=56.0 mol. The relative magnitude of R[111]A grew with decreasing [H_2O_2] and exceeded those of R[$\bar{1}\bar{1}\bar{1}$]B and R[110]. Consequently, γ even below unity, 0.9, was successfully realized. Table 1 also lists this high [H_2O] and low [H_2O_2] region in the last row. To our knowledge, this is the first etchant system that yields γ less than unity.

Finally, we would like to emphasize that an extensive control of etching anisotropy, expressed by γ ranging from 3.8 to 0.9, has successfully been achieved with H_2O_2-excess $HF+H_2O_2+H_2O$ mixtures by varying mainly [H_2O] and secondly [H_2O_2].

1-2. Etching profile

In this section, the etching profiles produced on four substrates is examined in terms of the intersection angle, θ_i (i=1, 2, --), of the side wall to the substrate surface and the control of θ_i by varying the mixture composition is presented. A side wall with an intersection angle θ_i is briefly referred to as "side wall θ_i" below.

Figures 4, 6, 8, and 10 show the variation of the [$\bar{1}$10] cross-sectional etching profiles and the top view of the intersection corners of the two orthogonal stripes with the mixture composition in (a)-(f), a schematic presentation of the profiles with defined θ_is in (g), and main low-index surfaces appearing as possible side walls in (h) for (001), (110), ($\bar{1}\bar{1}\bar{1}$)B, and (111)A substrates, respectively. Since the (001) substrate has two orthogonal cleavage planes, ($\bar{1}$10) and (110), the [110] cross-sectional etching profiles are also

shown in Figure 4. The etching profiles appearing on the two sides of a stripe were exactly the same for the (001) substrate but different for the other substrates due to the symmetry difference. Figures 5, 7, 9, and 11 summarize the variation of θ_is as a function of $[H_2O]$ for $\alpha=0.05/0.17$ in (a) and 0.05/0.34 in (b) and as a function of $[H_2O_2]$ for $[H_2O]=56.0$ mol in (c) for (001), (110), $(\bar{1}\bar{1}\bar{1})$B, and (111)A substrates, respectively. The etching behavior is summerized as follows.

(1) (001), (110), and $(\bar{1}\bar{1}\bar{1})$B substrates

1) For low $[H_2O]$ and high $[H_2O_2]$ mixtures, which give high γ, the three substrates exhibit their respective characteristic side wall profiles determined by the crystallographic anisotropy ((a) and (b) of Figures 4, 6, and 8).

① The (111)A-related side walls are θ_1, θ_3, θ_4, and θ_7, the $(\bar{1}\bar{1}\bar{1})$B-related side walls are θ_2, θ_5, and θ_9, and the (001)-related side walls are θ_6 and θ_8.

② The (111)A-related side walls have a flat slope and make a sharp intersection with other planes, while the $(\bar{1}\bar{1}\bar{1})$B- and (001)-related side walls have a curved slope and a round intersection with other planes [23].

③ A facet associated with the [101] or [011] orientation appears on the side that contains the (111)A-related side wall at the intersections of the two orthogonal stripes.

2) As $[H_2O]$ increases and/or $[H_2O_2]$ decreases, the θ_is all decrease and some of the side walls, θ_3, θ_6, and θ_9, disappear ((c) and (d) of Figures 4, 6, and 8).

① For the $(\bar{1}\bar{1}\bar{1})$B-related side walls θ_2 and θ_5 and the $(00\bar{1})$-related side walls θ_6 and θ_8, there exist regions of $[H_2O]$ and $[H_2O_2]$ where no definition of θ_i is possible, that is, $[H_2O]=2-3$ mol for $\alpha=0.05/0.17$ and $[H_2O]=7-15$ mol for $\alpha=0.05/0.34$.

② The facets at the intersections of the two orthogonal stripes diminish.

3) For high $[H_2O]$ and/or low $[H_2O_2]$ mixtures, which give low γ, the three substrates exhibit similar etching profiles characterized by smaller θ_is and

flat slopes reflecting no crystallographic anisotropy ((e) and (f) of Figures 4, 6, and 8).

① The $(\bar{1}\bar{1}\bar{1})$B-related side walls θ_2 and θ_5 and the $(00\bar{1})$-related side wall θ_8 also show a flat slope surface and a sharp intersection with the substrate planes, indistinguishable from the (111)A-related side walls θ_1, θ_4, and θ_7.

② The facets at the intersections of the two orthogonal stripes completely vanish.

(2) (111)A substrate (Figure 10)

1) In contrast to the $(\bar{1}\bar{1}\bar{1})$B and (110) substrates, the side walls on both sides of the $[\bar{1}10]$ stripe, θ_{10} and θ_{11}, maintain a flat slope and a sharp intersection with the (111)A plane irrespective of the values of θ_{10} and θ_{11} except for low $[H_2O]$ for which the slope surface is slightly curved.

2) The values of θ_{10} and θ_{11} decrease continuously as $[H_2O]$ increases and/or $[H_2O_2]$ decreases.

3) In contrast to the three other substrates, no facets are produced at the intersection corners of the two orthogonal stripes irrespective of $[H_2O]$ and $[H_2O_2]$.

The whole $HF+H_2O_2+H_2O$ mixture successfully achieved a wide-range control of θ_i as summarized in Table 2. The control ranges of θ_is extend up to 60 ° for the (001), (110), and $(\bar{1}\bar{1}\bar{1})$B substrates and 80 ° for the (111)A substrate, covering all main low- and high-index planes appearing as possible side walls.

1-3 Relation of etching profile with anisotropy of R

The orientation of a side wall is dominantly determined by the direction of the lowest R [24]. Since R[111]A is the lowest for most mixture compositions examined, the (111)A-related side walls are always produced on (001), (110), and $(\bar{1}\bar{1}\bar{1})$B substrates, that is, θ_1, θ_3, θ_4, and θ_7, and the corresponding θ_is are limited to the intersection angle of the (111)A plane to the substrate plane. The appearance of the facets at the intersections of the two or-

thogonal stripes for low [H_2O] indicated in (1)-1)-③ of the previous section can be attributed to the fact that R[111]A≪R[110]. Since the anisotropy weakens as [H_2O] increases and [H_2O_2] decreases, these facets accordingly disappear.

Then, the second lowest R is an important factor as well for determining θ_i not related to the (111)A plane. The order of magnitude of Rs in the three other orientations varies with [H_2O] and [H_2O_2] as shown in Table 1. For the (001) substrate, since R[$\bar{1}\bar{1}\bar{1}$]B is always the second lowest, the ($\bar{1}$11)B-related side wall θ_2 persists through the whole [H_2O] and [H_2O_2] range. For the (110) and ($\bar{1}\bar{1}\bar{1}$)B substrates, the second lowest R changes from R[001] to R[$\bar{1}\bar{1}\bar{1}$]B as [H_2O] increases. This well explains the result for the (110) substrate that the (00$\bar{1}$)-related side wall θ_6 disappears while the (11$\bar{1}$)B-related side wall θ_5 remains as [H_2O] increases and the presence of the (00$\bar{1}$)-related side wall θ_8 at low [H_2O] for the ($\bar{1}\bar{1}\bar{1}$)B substrate. The disappearance of the (11$\bar{1}$)B-related inverted mesa θ_9 with increasing [H_2O] just corresponds to the close magnitudes of R[$\bar{1}\bar{1}\bar{1}$]B and R[001] at medium [H_2O]. Actually, the totally curved side walls indicated in (1)-2)-① of the previous section are all produced in the medium [H_2O] region where R[110]≈R[$\bar{1}\bar{1}\bar{1}$]B≈R[001] (Table 1). For the (111)A substrate, the fact that R[111]A is the lowest leads to a lateral etching progress since the side walls are mainly composed of surfaces other than the (111)A surface. R[$\bar{1}\bar{1}\bar{1}$]B and R[001] are always the second lowest Rs for the side walls θ_{10} and θ_{11}, respectively. This leads to a conclusion that the side wall θ_{10} is dominated by the (11$\bar{1}$)B surface (high θ) for low [H_2O] and receives greater contribution from the (110) surface (low θ) as R[$\bar{1}\bar{1}\bar{1}$]B relatively grows with [H_2O]. This inspection qualitatively explains the experimental result. The flatness of the side wall θ_{10} may be supported by the slow vertical etching progress which puts the (11$\bar{1}$)B - (110) intersection out of the substrate surface. On the other hand, since the (001) surface is sandwiched by two equivalent (111)A sur-

faces at an acute angle, the side wall θ_{11} would always be dominated by the $(\bar{1}\bar{1}1)$A-related inverted mesa, which is contradictory to the observation. A careful inspection of Figure 10(h) leads us to speculate that high-index planes existing between the $(\bar{1}\bar{1}1)$A and (001) planes, $(\bar{1}\bar{1}2)$A, $(\bar{1}\bar{1}3)$A, and so on, which have Rs higher than R[111]A but *lower* than R[001] dominate θ_{11}. If we assume that the weight of contribution to θ_{11} shifts from the $(\bar{1}\bar{1}2)$A ($\theta=90.0°$) surface to higher-index $(\bar{1}\bar{1}N)$A surfaces (N=3, 4, -- ; lower θ) at the (111)A substrate surface together with an augumented contribution of the (001) surface as the anisotropy of R around the [111]A direction becomes weak with $[H_2O]$, this gives a qualitative explanation for the decrease in θ_{11} with $[H_2O]$. The slow vertical etching progress is again thought to exclude the appearance of the $(\bar{1}\bar{1}1)$A - $(\bar{1}\bar{1}N)$A intersection in the profile.

Finally, the isotropic etching characteristics showing a flat surface and a sharp intersection profile observed for high $[H_2O]$ and low $[H_2O_2]$ cannot be explained by the competition among Rs alone, which would produce a totally curved profile because the Rs have close values. Detailed experimental information of Rs in high-index directions is required to quantitatively explain the results.

1-4 Temperature dependence of R

The etching experiments were also done at 10 °C and 40 °C for the mixtures with $\alpha=0.05/0.17$ and $[H_2O]=1.2$ mol, 6.2 mol, and 56.2 mol in order to investigate the dependence of R on the etching temperature T. The results are shown in Figure 12. The dependence of R on T is expressed by the following equation:

$$R[lmn]X = R_0[lmn]X \times \exp(-E_a[lmn]X / R_cT), \qquad [1]$$

where $R_0[lmn]X$ is the etching rate at $T=\infty$, $E_a[lmn]X$ the activation energy, and R_c the gas constant. The values of R_0 and E_a evaluated for the four substrates are summarized in Table 3. The table shows that E_a varies depending on the mixture composition and that, for a fixed mixture composi-

tion, E_a[001], E_a[110], and $E_a[\bar{1}\bar{1}\bar{1}]$B have slightly different (especially for low [H_2O]) but similar values while E_a[111]A is larger than these three. This results in a decrease (an increase) in γ at higher (lower) T. For example, $\gamma<1$ can also be realized for $\alpha=0.05/0.17$ with [H_2O]=56.2 mol at T>30 °C. Thus, the etching temperature gives rise to similar effects on the etching anisotropy as the mixture composition.

1-5 Etching mechanism

The general etching mechanism for acid-oxidant-water type mixtures including the etching inactivity of the (111)A surface due to the absence of unshared electrons [25] is well understood [26]. In this respect, the present $HF+H_2O_2+H_2O$ mixture, with H_2O_2 acting as an oxidizer, HF as an oxide dissolver, and H_2O as a diluent, reveals etching characteristics common to previous mixtures within the framework of the general etching mechanism, except for γ less than unity for high [H_2O] and low [H_2O_2]. The orientation-dependent E_a shown in 1-4 and the etching depth proportional to the etching time indicate that a reaction-rate-limited etching proceeds in the present mixture and Table 3 shows that this etching process persists for a wide [H_2O] range.

It has been reported that HF selectively dissolves Ga oxides and partly reduces As oxides, leaving metallic As and As oxides on GaAs (001) surfaces [27,28]. It has also been reported that static H_2O preferentially dissolves As oxides and forms Ga oxides on GaAs (001) surfaces [27,29,30]. Therefore, the etching process of the present mixture will include (1) Ga oxide formation by H_2O_2 (and H_2O for high [H_2O]) and successive dissolusion by HF for surface Ga atoms and (2) As oxide formation by H_2O_2 and successive reduction by HF (and dissolution by H_2O for high [H_2O]) for surface As atoms.

1-6 Comparison with other mixture systems

It is helpful to discuss here the etching characteristics in comparison with those of other mixture systems.

(1) γ : Table 4 summarizes the values of γ and the etching rate order reported for other mixture systems. As to γ, the present mixture (Table 1) covers the γ range obtained for $H_2SO_4+H_2O_2+H_2O$, $H_3PO_4+H_2O_2+H_2O$, and $C_3H_4(OH)(COOH)_3+H_2O_2$. Based on the etching mechanism modeled in 1-5, two processes of (1) preferential Ga oxide formation by H_2O and successive removal by HF and (2) preferential As oxide removal by H_2O and etching-resistant As-covered surface production by HF will develop in high $[H_2O]$ and low $[H_2O_2]$ environments. These processes will enhance R[111]A and reduce R[$\bar{1}\bar{1}\bar{1}$]B. The realization of $\gamma<1$ for high $[H_2O]$ and low $[H_2O_2]$ can be well explained by the processes. Since it has been reported that etching in $H_2SO_4+H_2O_2+H_2O$ and $H_3PO_4+H_2O_2+H_2O$ leaves Ga-rich oxides on GaAs (001) surfaces [31], both H_2SO_4 and H_3PO_4 are considered to better dissolve As oxides. This results in the difficulty of obtaining $\gamma \leqq 1$ for these mixtures, consistent with the experimental results for $H_2SO_4+H_2O_2+H_2O$ [2]. $NH_4OH+H_2O_2+H_2O$ and Br_2+CH_3OH show higher γ. Further reduction of $[H_2O]$ or further increase in $[H_2O_2]$ in the present system will extend the γ range to such higher values.

(2) Etching rate order : According to the simple model on which the number of unshared electrons at the surface determines the etching activity, the order R[$\bar{1}\bar{1}\bar{1}$]B>R[001]≈R[110]>R[111]A results [25]. Table 4 tells us that except for R[111]A this does not always apply. Differences in chemical properties of the oxide dissolvers may be responsible for the variety in etching rate order. In reality, Table 1 shows that R[$\bar{1}\bar{1}\bar{1}$]B is *never* the highest for any composition of the present mixture and even the lowest for high $[H_2O]$ and low $[H_2O_2]$. HF as a selective Ga oxide dissolver [27,28] may be responsible for the relatively low R[$\bar{1}\bar{1}\bar{1}$]B. It should be noted that the relatively low magnitude of R[$\bar{1}\bar{1}\bar{1}$]B in the present mixture contributes to the clear appearance of the ($\bar{1}\bar{1}\bar{1}$)B-related side walls θ_2 and θ_5, in contrast to the complete absence of the ($\bar{1}\bar{1}\bar{1}$)B-related side walls in several other mixture sys-

tems [1-6,11] for which R[$\bar{1}\bar{1}\bar{1}$]B is the highest. Considering Figure 2, the ($\bar{1}\bar{1}\bar{1}$)B-related side walls should persist after a further reduction of [H_2O] or a further increase in [H_2O_2] in order to obtain higher γ in the present system.

(3) (111)A-related side walls : The intersection profile between the side wall and the substrate plane and between the neighboring side walls critically depends on the sharpness around the pertinent local minimum in a polar diagram for R as has been reported for $H_2SO_4+H_2O_2+H_2O$ [2,24]. Several popular mixture systems produce (111)A-related side walls having curved slopes and round intersection corners [2,4,5,11,12]. The presence of less sharp local minimums at R[111]A and other local minimums near R[111]A has been demonstrated for such profiles [2,7]. For the present mixture, the flat surface and sharp intersection profile obtained for the (111)A-related side walls and the side walls θ_{10} and θ_{11} throughout the whole composition range suggests the presence of a *prominently sharp* local minimum at R[111]A without other local minimums near R[111]A. The (001)- and ($\bar{1}\bar{1}\bar{1}$)B-related side walls showing a curved surface and a round intersection profile are caused by less sharp local minimums as with other mixture systems.

(4) Especially compared with popular $H_2SO_4+H_2O_2+H_2O$ [1,2,12], the present mixture is free from the heat generation during preparation and the high viscosity, hence it is much easier to use.

In order to fully understand the etching characteristics and elucidate etching mechanisms specific to the present mixture, close analyses of surface chemical reactions and resultant surface compositions are required.

2. <u>HF-excess mixtures (α=0.69/0.02 and 0.25/0.11)</u>

The mixture with α=0.69/0.02 showed very low Rs of the order of 10^{-2}~10^{-1} μm/min and a constant γ value of 1.7 in the whole [H_2O] range investigated. Moreover, the mixture with low [H_2O] eroded the etched patterns through penetration into the resist-substrate interface at the pattern edge

irrespective of the substrate orientation. Although the mixture with $\alpha = 0.25/0.11$ showed 5-fold enhanced R values and a variation of γ from 2.9 to 1.7 with [H_2O], the same erosion phenomenon was observed for low [H_2O]. Therefore, it is concluded that HF-excess mixtures are not suitable for selective etching. Excess HF may be responsible for such a patterning failure. $HF+H_2O_2+H_2O$ mixtures reported for revealing etch-pits [20,21] have more or less HF-excess compositions, hence they are not suitable for selective etching.

3. Application

The results obtained for H_2O_2-excess mixtures can be extensively applied to both basic material research and device fabrication. For example, mixtures with low [H_2O] and high [H_2O_2] showing strongly anisotropic etching characteristics are well suited for fabricating a variety of patterned substrates and microstructures with well-defined side walls (especially (111)A-related ones). Precise and wide-range controllability of the intersection angles can be applied to formation of and crystal growth on various high-index side walls. Mixtures with high [H_2O] and low [H_2O_2] showing isotropic etching characteristics can be used for surface treatments before crystal growth and for device processing, mesa-etching for device delineation and isolation, and recess etching for active layer thickness adjustments. The isotropic etching characteristics ensure the fabrication of devices in arbitrary orientations without modifying the designed structure and size.

We have not checked the etching characteristics of the present mixture on other related compounds such as AlGaAs. More complicated microstructures can be constructed by taking advantage of the possible etching rate difference among different compounds in combination with the orientation-dependent etching rate shown here.

IV. SUMMARY AND CONCLUSION

Selective etching characteristics of $HF+H_2O_2+H_2O$ mixtures have been examined for GaAs (111)A, $(\bar{1}\bar{1}\bar{1})$B, (001), and (110) surfaces. H_2O_2-excess mixtures showed excellent selective etching characteristics controlled by the H_2O and H_2O_2 contents. The anisotropy parameter, γ, ranged from 3.8 to 0.9 depending on the mixture composition. The etching rate is the slowest in the [111]A direction for most compositions, while the etching rate becomes the lowest in the $[\bar{1}\bar{1}\bar{1}]$B direction for high H_2O and low H_2O_2 concentrations. The lowest etching rate in directions other than [111]A has been realized with the present mixture system. Etching profiles strongly reflecting crystallographic anisotropy have been produced for low H_2O and high H_2O_2 concentrations, while those for high H_2O and low H_2O_2 concentrations have shown similar isotropic features irrespective of the substrate orientation. A continuous and extensive control of the intersection angle between the side wall and the substrate surface has been successfully achieved on all substrates. The etching profile has been found to be closely related to the degree of anisotropy of the etching rate and the contrast that the (111)A plane sharply intersects with other planes while the $(\bar{1}\bar{1}\bar{1})$B plane has a round intersection profile. The etching mechanism has been discussed on a model that HF acts as a selective Ga oxide dissolver and H_2O as a preferential As oxide dissolver. Special features of the present mixture have been highlighted in comparison with other mixture systems. HF-excess mixtures have been found to be unsuitable for selective etching of GaAs because of excessively low etching rates and erosion of etched patterns.

-ACKNOWLEDGMENTS-

The authors would like to thank Dr. Y. Furuhama, President of ATR Optical and Radio Communications Research Laboratories, for his encouragement throughout this work.

-REFERENCES-

1) S. Iida and K. Ito, J. Electrochem. Soc. 118, 768 (1971).

2) D. W. Shaw, J. Electrochem. Soc. 128, 874 (1981).

3) J. J. Gannon and C. J. Nuese, J. Electrochem. Soc. 121, 1215 (1974).

4) S. H. Jones and D. K. Walker, J. Electrochem. Soc. 137, 1653 (1990).

5) Y. Mori and N. Watanabe, J. Electrochem. Soc. 125, 1510 (1978).

6) Y. Tarui, Y. Komiya, and Y. Harada, J. Electrochem. Soc. 118, 118 (1971).

7) L. A. Koszi and D. L. Rode, J. Electrochem. Soc. 122, 1676 (1975).

8) B. Tuck, J. S. K. Mills, and A. J. Hartwill, J. Mater. Sci. 11, 847 (1976).

9) H. P. Meier, E. van Gieson, R. F. Broom, W. Walter, D. J. Webb, Ch. Harder, and H. Jäckel, Inst. Phys. Conf. Ser. No.91, 609 (1987).

10) H. P. Meier, R. F. Broom, P. W. Epperlein, E. van Gieson, Ch. Harder, H. Jäckel, W. Walter, and D. J. Webb, J. Vac. Sci. Technol. B 6, 692 (1988).

11) M. Otsubo, T. Oda, H. Kumabe, and H. Miki, J. Electrochem. Soc. 123, 676 (1976).

12) S. Adachi and K. Oe, J. Electrochem. Soc. 130, 2427 (1983).

13) For (110) substrates, for example, J. M. Ballingall and C. E. C. Wood, Appl. Phys. Lett. 41, 947 (1982); L. T. P. Allen, E. R. Weber, J. Washburn, and Y. C. Pao, Appl. Phys. Lett. 51, 670 (1987); M. Sato, K. Maehashi, H. Asahi, S. Hasegawa, and H. Nakashima, Superlattices and Microstructures 7, 279 (1990).

14) For $(\bar{1}\bar{1}\bar{1})$B substrates, for example, T. Hayakawa, M. Kondo, T. Suyama, K. Takahashi, S. Yamamoto, and T. Hijikata, Jpn. J. Appl. Phys. 26, L302 (1987); A. Chin, P. Martin, P. Ho, J. Ballingall, T. Yu, and J. Mazurowski, Appl. Phys. Lett. 59, 1899 (1991); T. Fukui, S. Ando, Y. Tokura, and T. Toriyama, Appl. Phys. Lett. 58, 2018 (1991).

15) For (111)A substrates, for example, Y. Okano, M. Shigeta, H. Seto, H. Katahama, S. Nishine, and I. Fujimoto, Jpn. J. Appl. Phys. **29**, L1357 (1990); Y. Kadoya, A. Sato, H. Kano, and H. Sakaki, J. Cryst. Growth **111**, 280 (1991); T. Yamamoto, M. Fujii, T. Takebe, D. Lovell, and K. Kobayashi, Inst. Phys. Conf. Ser. No. **120**, 31 (1991).

16) For high-index substrates, for example, W. I. Wang, E. E. Mendez, T. S. Kuan, and L. Esaki, Appl. Phys. Lett. **47**, 826 (1985); S. Subbanna, H. Kroemer, and J. L. Merz, J. Appl. Phys. **59**, 488 (1986); P. N. Uppal, J. S. Ahearn, and D. P. Musser, J. Appl. Phys. **62**, 3766 (1987); K. Mochizuki, S. Goto, and C. Kusano, Appl. Phys. Lett. **58**, 2939, (1991); W. Q. Li and P. K. Bhattacharya, S. H. Kwok, and R. Merlin, J. Appl. Phys. **72**, 3129 (1992).

17) For (001) patterned substrates, for example, D. L. Miller, Appl. Phys. Lett. **47**, 1309 (1985); References 9 and 10; E. Kapon, D. M. Hwang, M. Walther, R. Bhat, and N. G. Stoffel, Surface Science **267**, 593 (1992); S. Shimomura, S. Ohkubo, Y. Yuba, S. Namba, S. Hiyamizu, M. Shigeta, T. Yamamoto, and K. Kobayashi, Surface Science **267**, 13 (1992).

18) For $(\bar{1}\bar{1}\bar{1})$B patterned substrates, for example, Y. Nomura, Y. Morishita, S. Goto, Y. Katayama, and T. Isu, Jpn. J. Appl. Phys. **30**, 3771 (1991).

19) For (111)A patterned substrates, for example, M. Fujii, T. Yamamoto, M. Shigeta, T. Takebe, K. Kobayashi, S. Hiyamizu, and I. Fujimoto, Surface Science **267**, 26 (1992); T. Takebe, M. Fujii, T. Yamamoto, K. Fujita, and K. Kobayashi, presented at the 7th International Conference on Molecular Beam Epitaxy (24-28 August 1992; Schwäbisch Gmünd).

20) J. L. Richards and A. J. Crocker, J. Appl. Phys. **31**, 611 (1960).

21) J. Nishizawa, Y. Oyama, H. Tadano, K. Inokuchi, and Y. Okuno, J. Cryst. Growth **47**, 434 (1979).

22) The conversion of units from cc to mol was made according to the following equations :

[HF] (mol) = 0.0245 × [46 wt. % HF] (cc),

[H_2O_2] (mol) = 0.0107 × [35 wt. % H_2O_2] (cc),

[H_2O] (mol) = 0.0319 × [46 wt. % HF] (cc) + 0.0374 × [35 wt. % H_2O_2] (cc) + 0.0556 × [H_2O] (cc).

23) The etching profiles along the side wall θ_2 - the (001) substrate plane, along the side wall θ_6 - the side wall θ_5 - the (110) substrate plane, and along the side wall θ_9 - the side wall θ_8 - the $(\bar{1}\bar{1}\bar{1})$B substrate plane were the same. This result and the (111)A-related side walls showing the flat surface and sharp intersection profile ensure that the obtained profiles are not influenced by the resist or substrate orientation. These also served for unambiguous identifcation of the side wall orientations in this work.

24) D. W. Shaw, J. Cryst. Growth **47**, 509 (1979).

25) H. C. Gatos and M. C. Levine, J. Electrochem. Soc. **107**, 427 and 433 (1960).

26) For example, R. E. Williams, "Gallium Arsenide Processing Techniques" (Artech House, Inc., Dedham; 1984), Chap. 5.

27) D. Gräf, M. Grundner, D. Lüdecke, and R. Schulz, J. Vac. Sci. Technol. A **8**, 1955 (1990).

28) K. Menda, E. Kanda, and T. Yokoyama, Jpn. J. Appl. Phys. **29**, L391 (1990).

29) B. Schwartz, J. Electrochem. Soc. **118**, 657 (1971).

30) J. Massies and J. P. Contour, Appl. Phys. Lett. **46**, 1150 (1985).

31) Z. H. Lu, C. Lagarde, E. Sacher, J. F. Currie, and A. Yelon, J. Vac. Sci. and Technol. A **7**, 646 (1989).

-FIGURE CAPTIONS-

Figure 1 Variation of the etching rate R and the etching anisotropy γ with the H_2O content for (a) $\alpha=0.05/0.17$ and (b) $\alpha=0.05/0.34$.

Figure 2 Variation of the normalized etching rate with the H_2O content for (a) $\alpha=0.05/0.17$ and (b) $\alpha=0.05/0.34$.

Figure 3 Variation of (a) the etching rate R and the etching anisotropy γ and (b) the normalized etching rate with the H_2O_2 content for HF content of 0.05 mol and H_2O content of 56.0 mol.

Figure 4 Variation of the etching profiles with the mixture composition for the (001) substrate.

Figure 5 Variation of the slopes of the side walls with the H_2O content, (a) and (b), and with the H_2O_2 content, (c), for the (001) substrate. Open and filled symbols represent normal and inverted mesas, respectively. Symbols at $\theta=0°$ mean disappearance of the corresponding side walls. Two symbols and a vertical bar connecting them mean that the corresponding side wall has a slope ranging between the two symbols.

Figure 6 Variation of the etching profiles with the mixture composition for the (110) substrate.

Figure 7 Variation of the slopes of the side walls with the H_2O content, (a) and (b), and with the H_2O_2 content, (c), for the (110) substrate. Symbols at $\theta=0°$ mean disappearance of the corresponding side walls.

Figure 8 Variation of the etching profiles with the mixture composition for the $(\bar{1}\bar{1}\bar{1})$B substrate.

Figure 9 Variation of the slopes of the side walls with the H_2O content, (a) and (b), and with the H_2O_2 content, (c), for the $(\bar{1}\bar{1}\bar{1})$B substrate. Open and filled symbols represent normal and inverted mesas, respectively. Symbols at $\theta=0°$ mean disappearance of the

corresponding side walls. Two symbols and a vertical bar connecting them mean that the corresponding side wall has a slope ranging between the two symbols.

Figure 10 Variation of the etching profiles with the mixture composition for the (111)A substrate.

Figure 11 Variation of the slopes of the side walls with the H_2O content, (a) and (b), and with the H_2O_2 content, (c), for the (111)A substrate. Two symbols and a vertical bar connecting them mean that the corresponding side wall has a slope ranging between the two symbols.

Figure 12 Dependence of the etching rate R and the etching anisotropy γ on the etching temperature T for $\alpha = 0.05/0.17$ with H_2O contents of 1.2, 6.2, and 56.2 mol.

-TABLE HEADINGS-

Table 1 Summary of the values of γ and the etching rate order in the four regions defined for the present mixture.

Table 2 Summary of the slopes of the side walls controlled by the present mixture and related main low- and high-index planes.

Table 3 Summary of the values of parameters R_0 and E_a obtained for $\alpha = 0.05/0.17$ on the four substrates.

Table 4 List of the values of γ and the etching rate reported for various mixture systems.

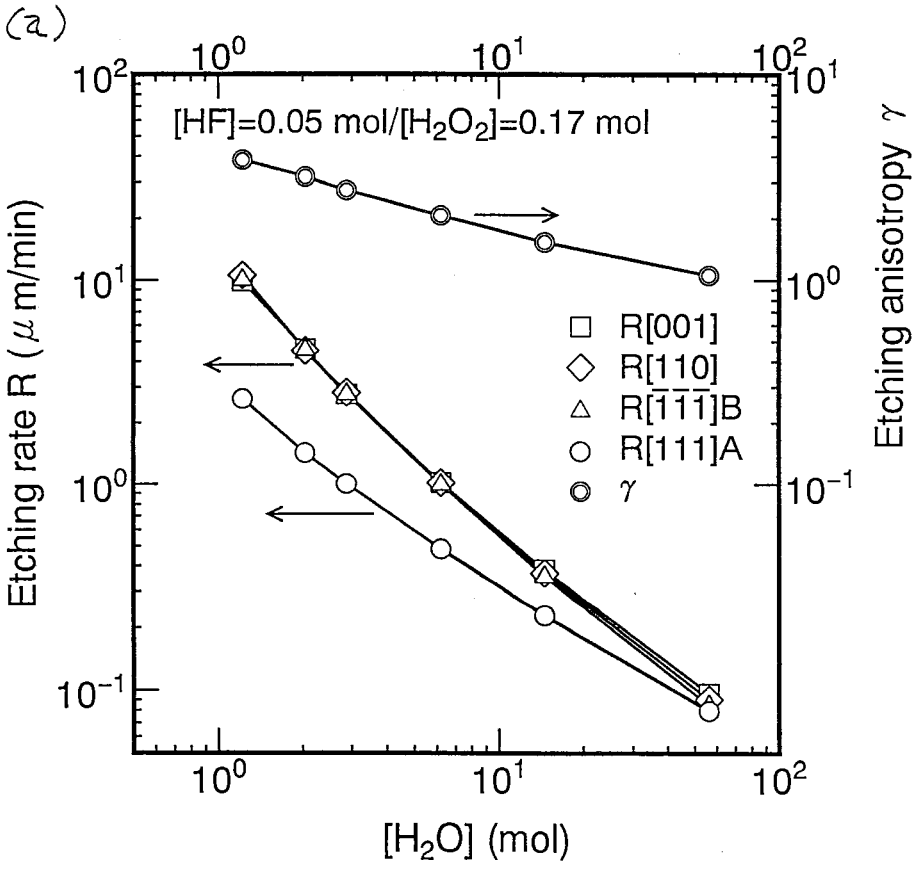

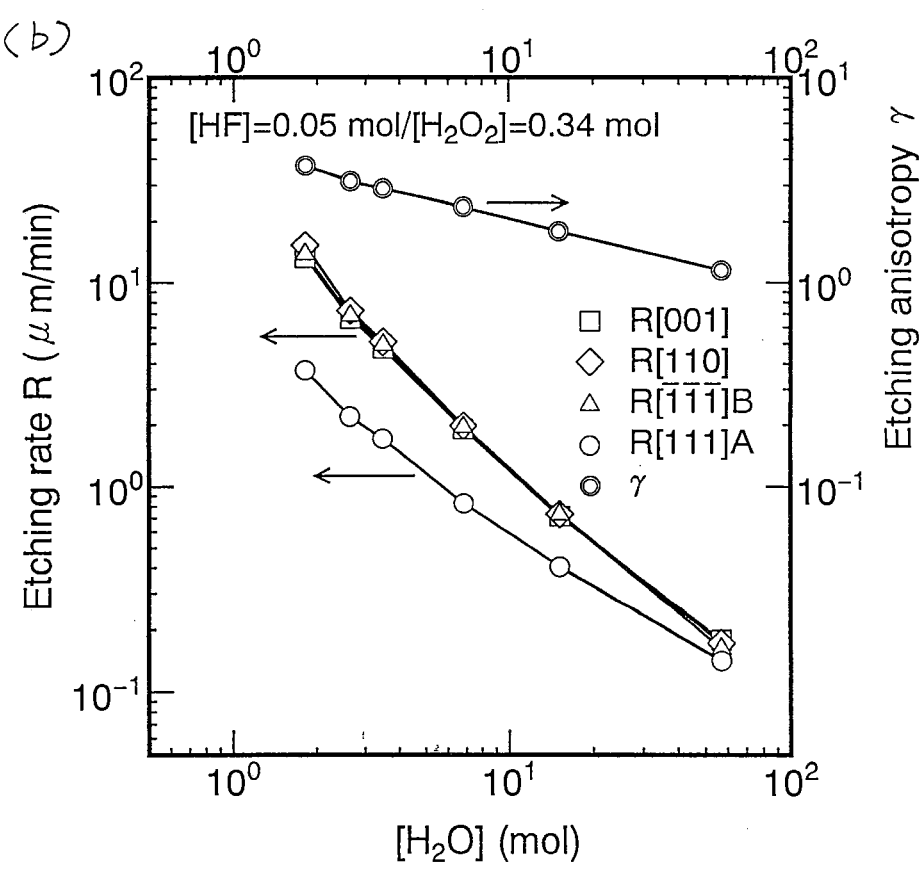

Figure 1 Variation of the etching rate R and the etching anisotropy γ with the H_2O content for (a) α=0.05/0.17 and (b) α=0.05/0.34.

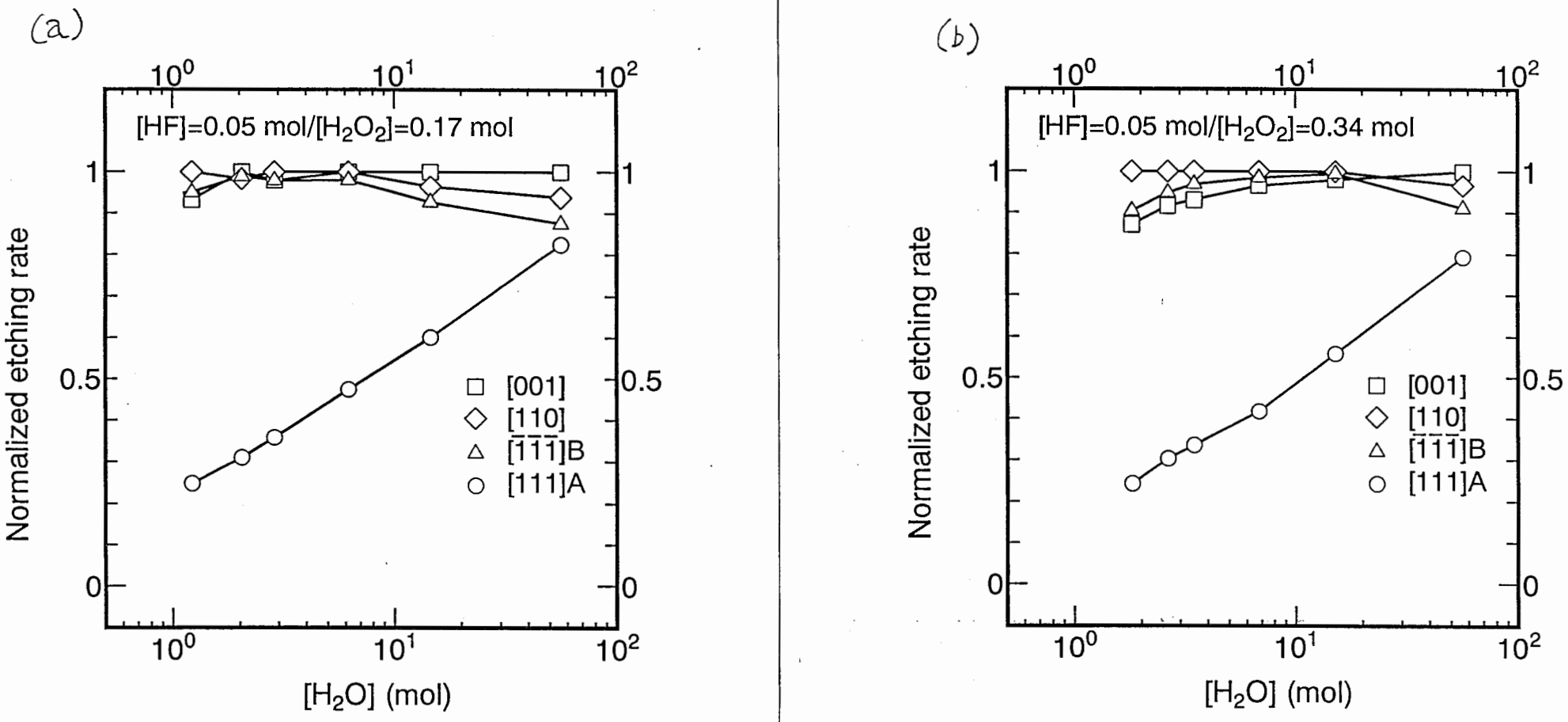

Figure 2 Variation of the normalized etching rate with the H_2O content for (a) $\alpha=0.05/0.17$ and (b) $\alpha=0.05/0.34$.

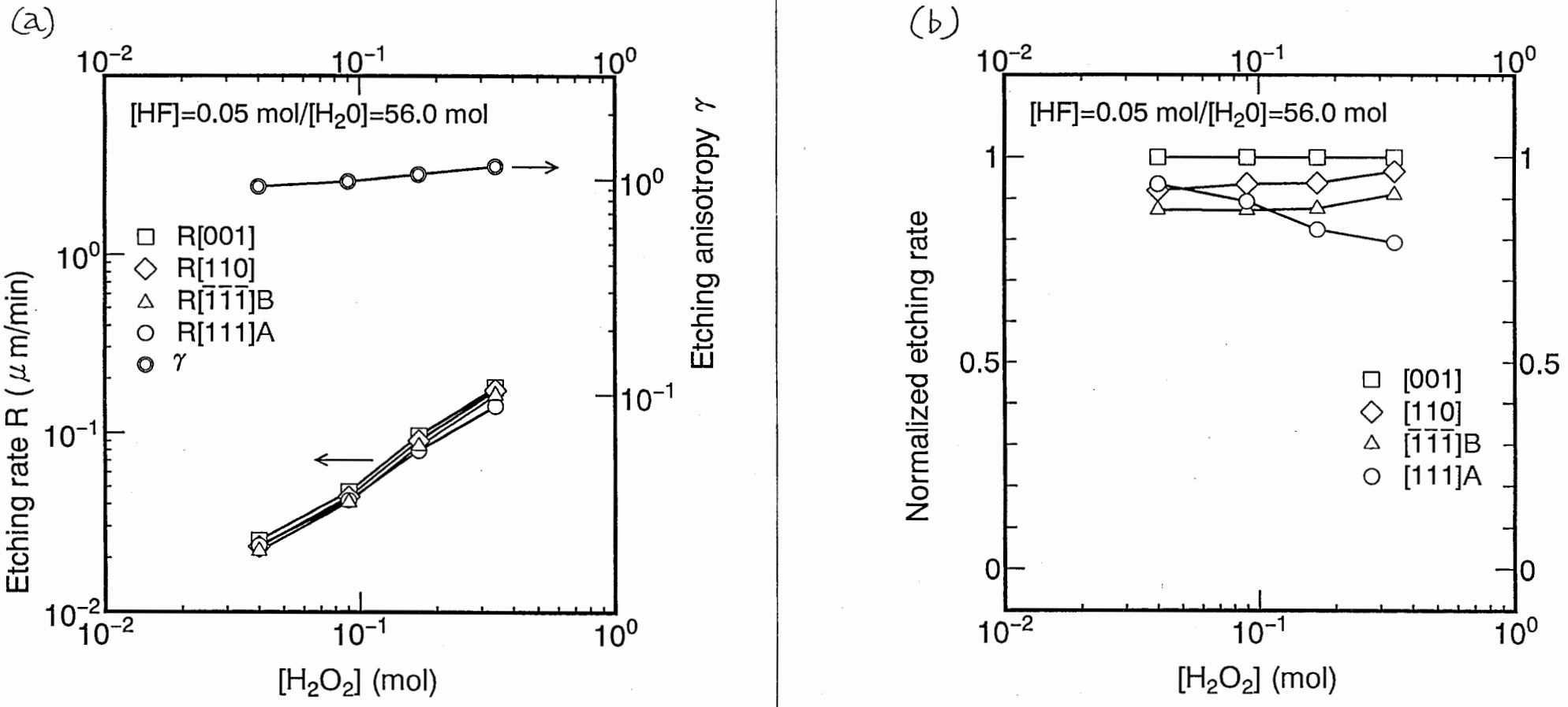

Figure 3 Variation of (a) the etching rate R and the etching anisotropy γ and (b) the normalized etching rate with the H_2O_2 content for HF content of 0.05 mol and H_2O content of 56.0 mol.

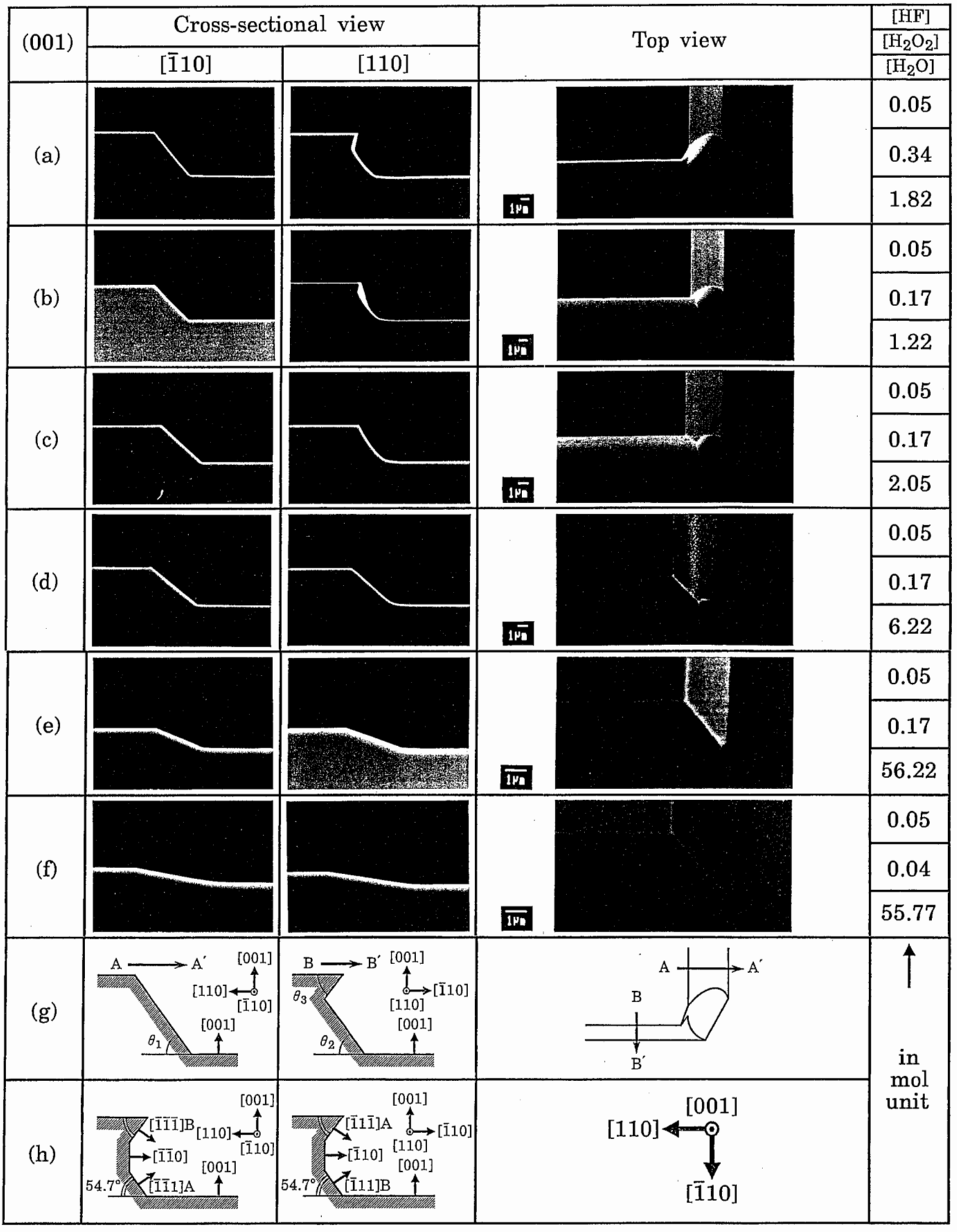

Figure 4 Variation of the etching profiles with the mixture composition for the (001) substrate.

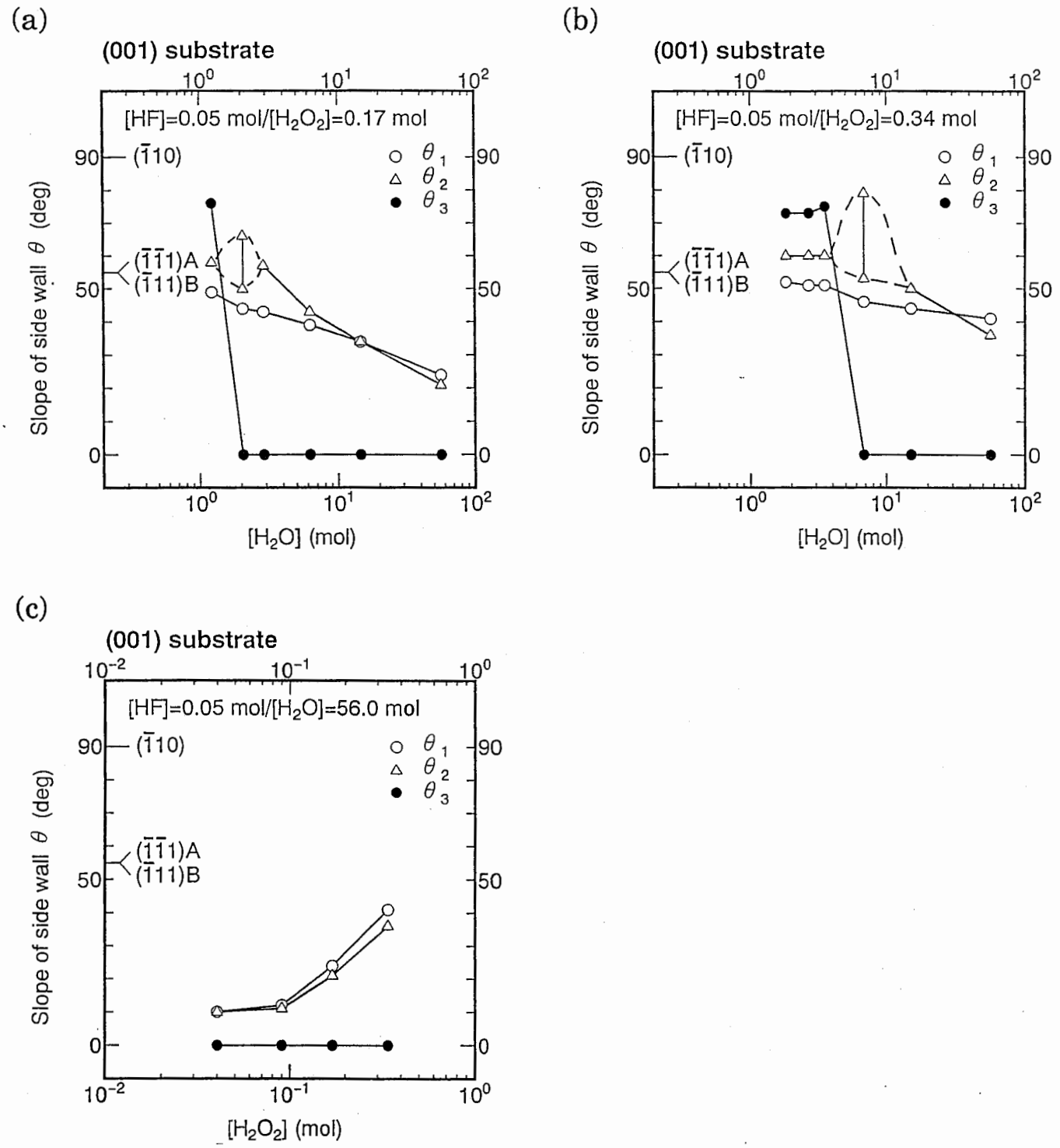

Figure 5 Variation of the slopes of the side walls with the H_2O content, (a) and (b), and with the H_2O_2 content, (c), for the (001) substrate. Open and filled symbols represent normal and inverted mesas, respectively. Symbols at $\theta = 0°$ mean disappearance of the corresponding side walls. Two symbols and a vertical bar connecting them mean that the corresponding side wall has a slope ranging between the two symbols.

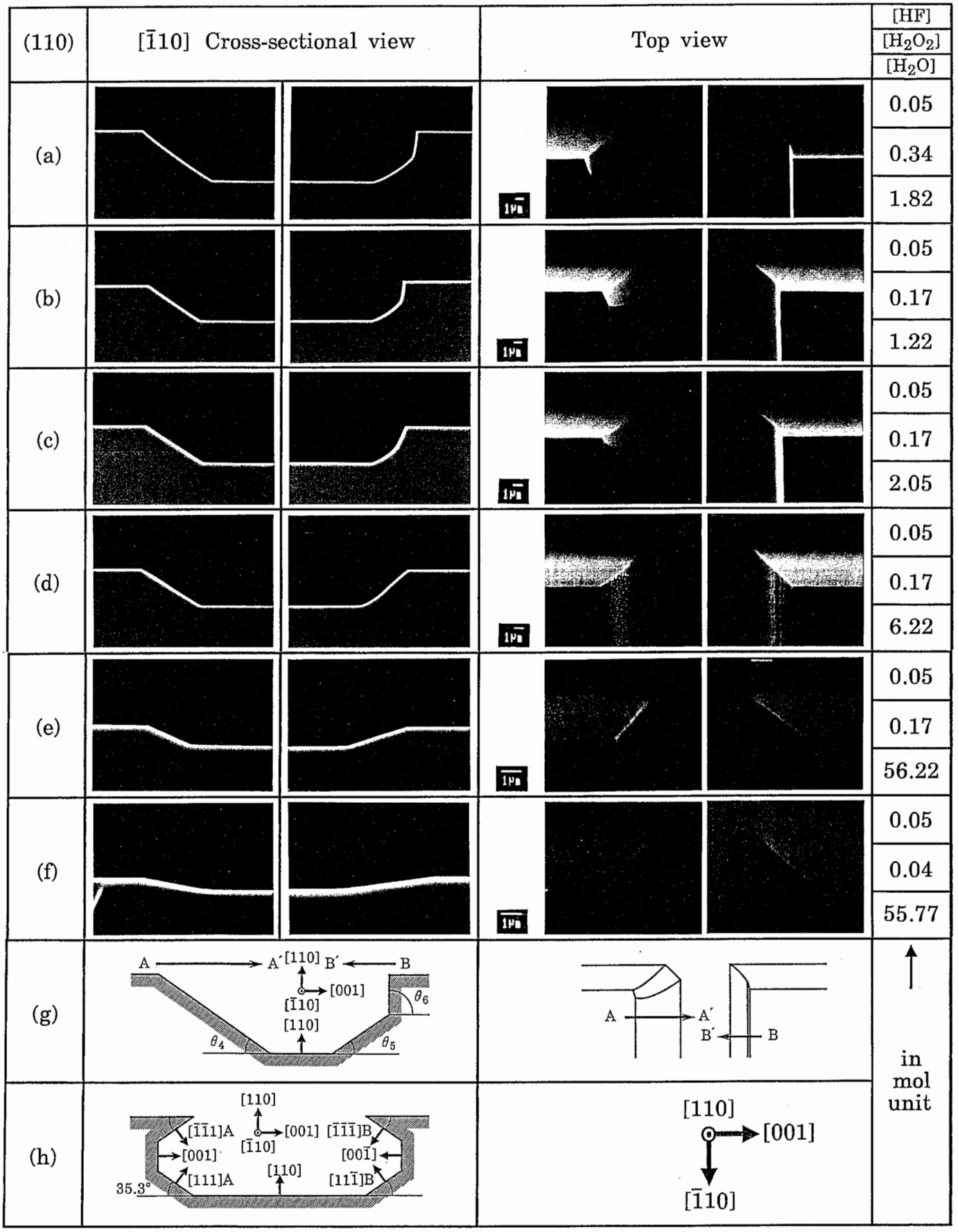

Figure 6 Variation of the etching profiles with the mixture composition for the (110) substrate.

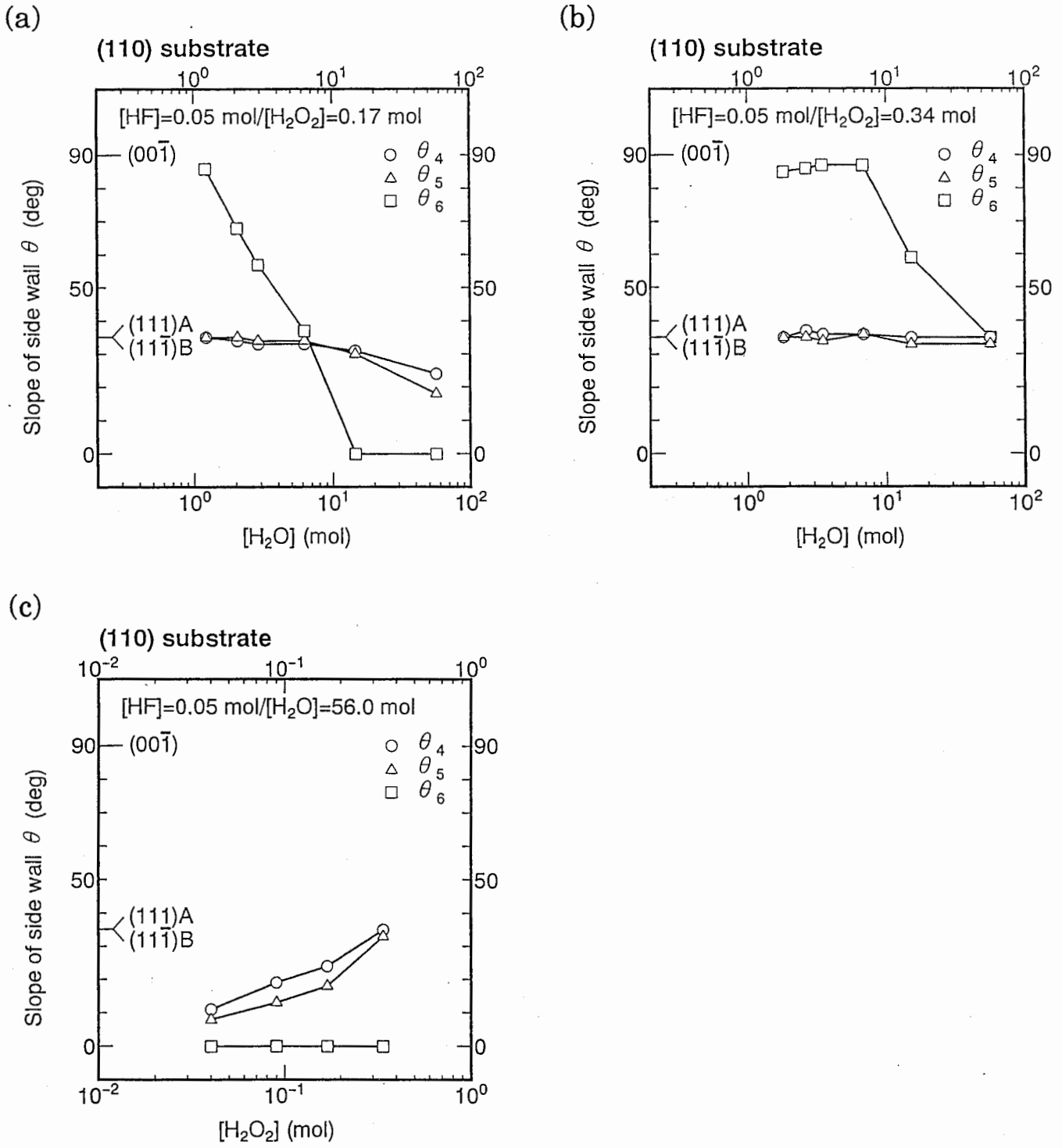

Figure 7 Variation of the slopes of the side walls with the H_2O content, (a) and (b), and with the H_2O_2 content, (c), for the (110) substrate. Symbols at $\theta = 0°$ mean disappearance of the corresponding side walls.

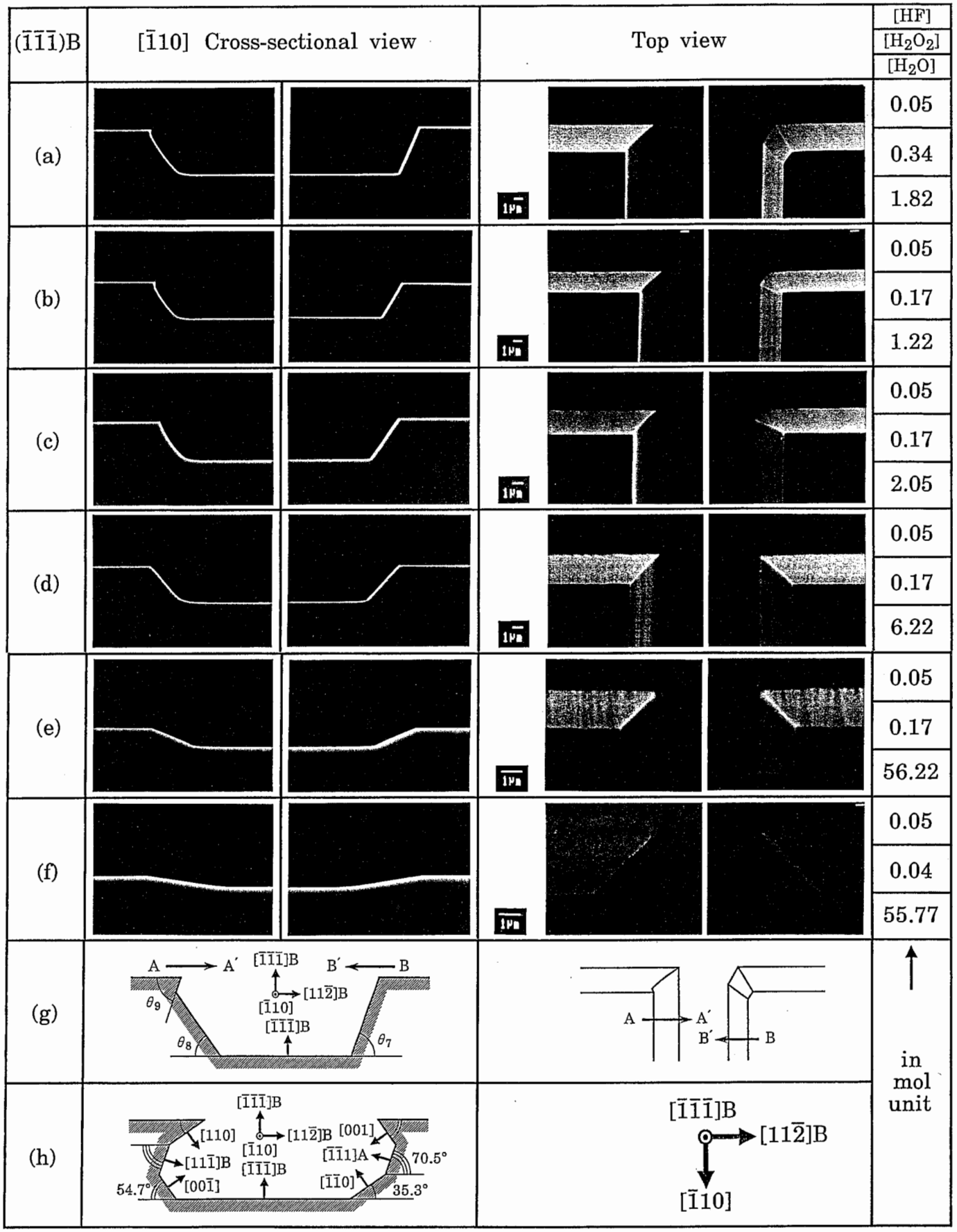

Figure 8 Variation of the etching profiles with the mixture composition for the $(\bar{1}\bar{1}\bar{1})$B substrate.

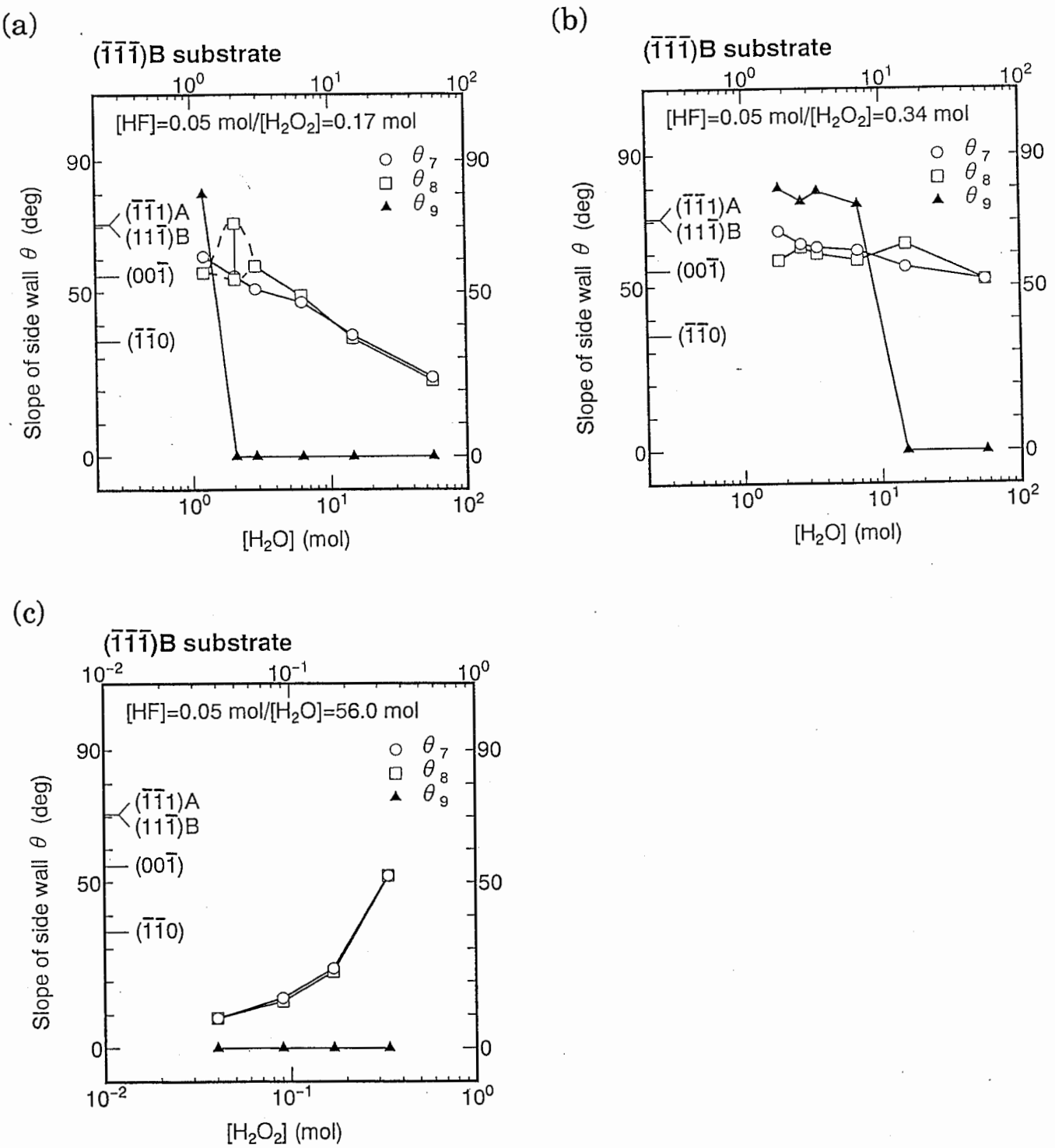

Figure 9 Variation of the slopes of the side walls with the H_2O content, (a) and (b), and with the H_2O_2 content, (c), for the $(\bar{1}\bar{1}\bar{1})$B substrate. Open and filled symbols represent normal and inverted mesas, respectively. Symbols at $\theta = 0°$ mean disappearance of the corresponding side walls. Two symbols and a vertical bar connecting them mean that the corresponding side wall has a slope ranging between the two symbols.

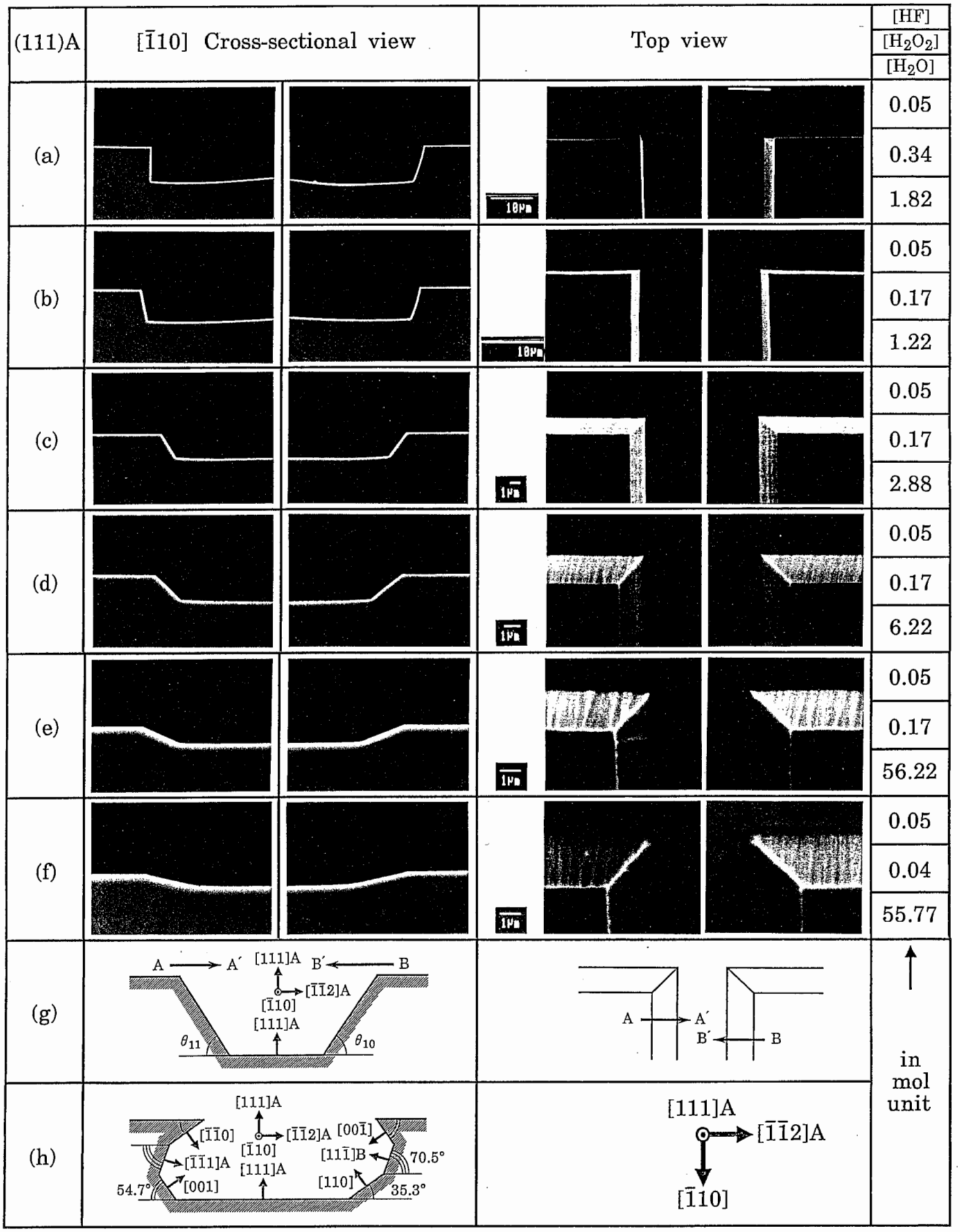

Figure 10 Variation of the etching profiles with the mixture composition for the (111)A substrate.

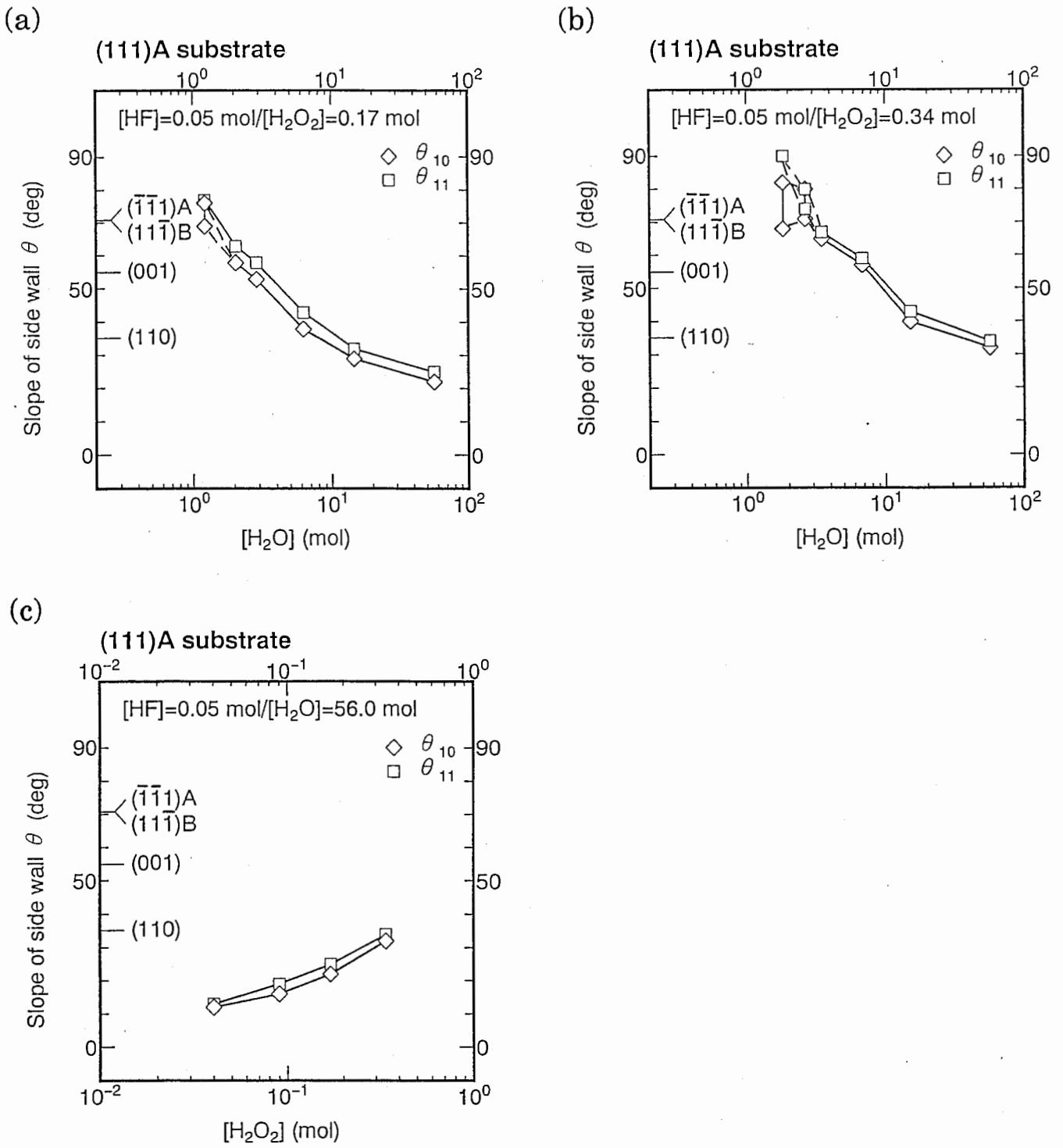

Figure 11 Variation of the slopes of the side walls with the H_2O content, (a) and (b), and with the H_2O_2 content, (c), for the (111)A substrate. Two symbols and a vertical bar connecting them mean that the corresponding side wall has a slope ranging between the two symbols.

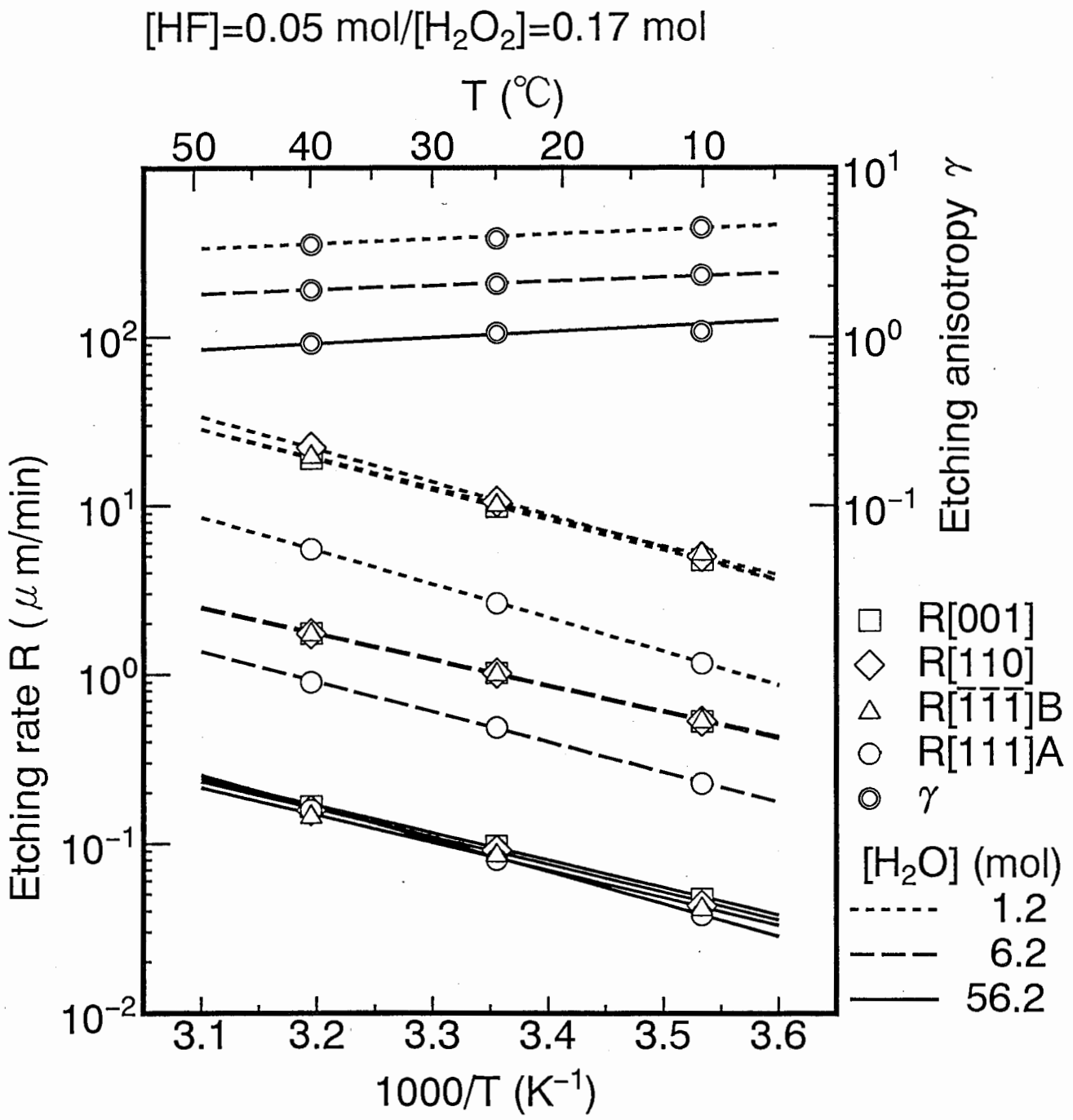

Figure 12 Dependence of the etching rate R and the etching anisotropy γ on the etching temperature T for α=0.05/0.17 with H_2O contents of 1.2, 6.2, and 56.2 mol.

Region criteria	Mixture composition (mol)			γ	Etching rate order
	[HF]	[H_2O_2]	[H_2O]		
Low [H_2O] and high [H_2O_2]	0.05	0.34	1.8 - 6.0	3.7 - 2.4	R[110] > R[$\bar{1}\bar{1}\bar{1}$]B > R[001] ≫ R[111]A
		0.17	1.2 - 1.5	3.8 - 3.5	
Medium [H_2O] and high [H_2O_2]		0.34	6.0 - 30.0	2.4 - 1.4	R[110] ≈ R[$\bar{1}\bar{1}\bar{1}$]B ≈ R[001] ≫ R[111]A
		0.17	1.5 - 10.0	3.5 - 1.4	
High [H_2O] and high [H_2O_2]		0.34	30.0 - 56.8	1.4 - 1.2	R[001] > R[110] > R[$\bar{1}\bar{1}\bar{1}$]B > R[111]A
		0.17	10.0 - 56.2	1.4 - 1.1	
High [H_2O] and low [H_2O_2]		0.09	56.0	1.0	R[001] > R[110] > R[111]A ≧ R[$\bar{1}\bar{1}\bar{1}$]B
		0.04		0.9	R[001] > R[111]A ≧ R[110] > R[$\bar{1}\bar{1}\bar{1}$]B

Table 1 Summary of the values of γ and the etching rate order in the four regions defined for the present mixture.

Substrate orientation	θ_i	Controlled range	Main low- and high-index planes / $\theta^{\#}$
(001)	θ_1	52° - 10°	$(\bar{1}\bar{1}1)$A / 54.7°, $(\bar{1}\bar{1}N)$A (N=2,3,--)
	θ_2	60° - 10°	$(\bar{1}11)$B / 54.7°, $(\bar{1}1N)$B (N=2,3,--)
	θ_3*	~ 73°	$(\bar{1}1\bar{1})$A / 54.7°
(110)	θ_4	35° - 8°	(111)A / 35.3°, (NN1)A (N=2,3,--)
	θ_5	36° - 11°	$(11\bar{1})$B / 35.3°, $(NN\bar{1})$B (N=2,3,--)
	θ_6	88° - 37°	$(00\bar{1})$ / 90.0°, $(11\bar{N})$B (N=2,3,--)
$(\bar{1}\bar{1}\bar{1})$B	θ_7	67° - 9°	$(\bar{1}\bar{1}1)$A / 70.5°, $(\bar{N}\bar{N}1)$A (N=2,3,--), $(\bar{1}\bar{1}0)$ / 35.3°, $(\bar{N}\bar{N}\bar{1})$B (N=2,3,--)
	θ_8	63° - 9°	$(00\bar{1})$ / 54.7°, $(\bar{1}\bar{1}\bar{N})$B (N=2,3,--)
	θ_9*	~ 78°	$(11\bar{1})$B / 70.5°
(111)A	θ_{10}	(82 - 68)° - 12°	$(11\bar{1})$B / 70.5°, $(NN\bar{1})$B (N=2,3,--), (110) / 35.3°, (NN1)A (N=2,3,--)
	θ_{11}	90° - 13°	$(\bar{1}\bar{1}2)$A / 90.0°, $(\bar{1}\bar{1}N)$A (N=3,4,--), (001) / 54.7°, (11N)A (N=2,3,--)

* Inverted mesa, # Angle to substrate plane

Table 2 Summary of the slopes of the side walls controlled by the present mixture and related main low- and high-index planes.

Substrate orientation	Parameter	[H_2O]		
		1.2 mol	6.2 mol	56.2 mol
(001)	R_0 (μm/min)	1.05×10^7	1.36×10^5	2.53×10^4
	E_a (kcal/mol)	8.22	6.99	7.41
(110)	R_0	3.42×10^7	1.57×10^5	2.74×10^4
	E_a	8.86	7.09	7.48
$(\bar{1}\bar{1}\bar{1})$B	R_0	6.08×10^6	1.41×10^5	2.27×10^4
	E_a	7.87	7.04	7.43
(111)A	R_0	1.22×10^7	4.52×10^5	2.02×10^5
	E_a	9.09	8.15	8.72

Table 3 Summary of the values of parameters R_0 and E_a obtained for $\alpha = 0.05/0.17$ on the four substrates.

Mixture	γ	Etching rate order [$]	Mixture composition	Ref.
$H_2SO_4+H_2O_2+H_2O$	3.8	$R[\bar{1}\bar{1}\bar{1}]B>R[001]\approx R[110]$	$[H_2SO_4]:[H_2O_2]:[H_2O]=1:8:1$	1
	1.9		$[H_2SO_4]:[H_2O_2]:[H_2O]=8:1:1$	
	4.2 - 2.1	$R[\bar{1}\bar{1}\bar{1}]B>R[001]>R[110]$	$[H_2SO_4]:[H_2O_2]:[H_2O]=1:8:1\sim80$	2
	1.5	$R[\bar{1}\bar{1}\bar{1}]B\approx R[001]>R[110]$	$[H_2SO_4]:[H_2O_2]:[H_2O]=1:8:160$	
$H_3PO_4+H_2O_2+H_2O$	3.0	$R[110]>R[\bar{1}\bar{1}\bar{1}]B>R[001]$	$[H_3PO_4]:[H_2O_2]:[H_2O]=1:9:1$	5
	2.0	$R[\bar{1}\bar{1}\bar{1}]B>R[110]>R[001]$	$[H_3PO_4]:[H_2O_2]:[H_2O]=7:3:3$	
	1.9	$R[110]>R[001]>R[\bar{1}\bar{1}\bar{1}]B$	$[H_3PO_4]:[H_2O_2]:[H_2O]=1:9:210,\ 3:1:50$	
$C_3H_4(OH)(COOH)_3+H_2O_2$	1.7	$R[\bar{1}\bar{1}\bar{1}]B>R[001]$	$[C_3H_4(OH)(COOH)_3]/[H_2O_2]=10$	11
$NH_4OH+H_2O_2+H_2O$	5.4	$R[\bar{1}\bar{1}\bar{1}]B>R[001]$	$[NH_4OH]:[H_2O_2]:[H_2O]=20:7:973$	3
	#	$R[\bar{1}\bar{1}\bar{1}]B>R[001]$	$[NH_4OH]:[H_2O_2]:[H_2O]=1:1:8$	4
Br_2+CH_3OH	9.2 - 3.0	$R[110]>R[\bar{1}\bar{1}\bar{1}]B>R[001]$	$[Br_2]/[CH_3OH]=0.01\sim0.05$ *	6

No data reported. [$] R[111]A is always the lowest. * Weight ratio. Otherwise, volume ratio.

Table 4 List of the values of γ and the etching rate reported for various mixture systems.